Autoproteolysis in *hedgehog* Protein Biogenesis

John J. Lee, Stephen C. Ekker, Doris P. von Kessler, Jeffery A. Porter, Benjamin I. Sun, Philip A. Beachy*

Extracellular signaling proteins encoded by the *hedgehog* (*hh*) multigene family are responsible for the patterning of a variety of embryonic structures in vertebrates and invertebrates. The *Drosophila hh* gene has now been shown to generate two predominant protein species that are derived by an internal autoproteolytic cleavage of a larger precursor. Mutations that reduced the efficiency of autoproteolysis in vitro diminished precursor cleavage in vivo and also impaired the signaling and patterning activities of the HH protein. The two HH protein species exhibited distinctive biochemical properties and tissue distribution, and these differences suggest a mechanism that could account for the long- and short-range signaling activities of HH in vivo.

The *hedgehog* (*hh*) gene of *Drosophila* was initially identified as a locus that is required for the establishment of polarity within embryonic segments (*1*). Later studies of genetic mosaics within imaginal disks, which are the larval precursors of adult structures, demonstrated that loss of *hh* function in a discrete patch of cells could affect the patterning of structures formed from adjacent wild-type cells (*2*). These nonautonomous patterning defects suggested that *hh* functions in an extracellular signaling pathway. Consistent with a role in extracellular signaling, HH protein undergoes signal-sequence cleavage when translated in the presence of microsomes (*3*) and regions of embryos that express the *hh* transcript are a subset of the spatial domains that are affected by *hh* mutations (*3–6*). Secretion of the HH protein has also been confirmed by antibody studies that demonstrate a broader distribution for *hh*-encoded antigens than for the *hh* transcript (*7*, *8*).

Studies with the *Drosophila* gene and its vertebrate homologs reinforce the conclusion that *hh* gene products function in extracellular signaling and that they induce gene expression and direct the formation of morphological pattern within structures adjacent to regions in which they are expressed (*9–15*). A puzzling feature of *hh* activity in these systems, however, has been the short-range nature of *hh*-dependent signaling in some contexts (*16*), whereas in other settings, *hh* activity appears to extend many cell diameters beyond the site of *hh* gene expression (*17*). Furthermore, the active form of the HH protein has not been identified in any of these systems. We focus here on the biogenesis of *Drosophila* HH protein (or proteins) active in signaling, and on the possibility that multiple forms of the HH protein may act in vivo.

The authors are in the Howard Hughes Medical Institute, Department of Molecular Biology and Genetics, The Johns Hopkins School of Medicine, Baltimore, MD 21205, USA.

*To whom correspondence should be addressed.

Early in vitro translation experiments showed that, in addition to signal-sequence cleavage, the full-length HH protein also appears to be further processed by cleavage at an internal location (*3*). This internal cleavage was not observed on translation in vitro of a form of the protein missing 61 amino acid residues at the COOH-terminus, and we proposed that this truncation might damage a domain involved in autoproteolysis. To more clearly define the products of this internal cleavage event and to identify HH protein products in vivo, we generated polyclonal antibodies to residues 83 to 160 (Ab1) and residues 300 to 391 (Ab2). We have used these antibodies for immunoblotting and for the immunoprecipitation of proteins from various sources including (i) in vitro translation extracts programmed with *hh* coding sequences and (ii) protein extracts from embryos, from imaginal disks, and from the *Drosophila* S2 (Schneider 2) cultured cell line stably transfected with an expression construct inducible for expression of HH protein. The following summary of these data outlines the formation of the predominant forms of the HH protein.

HH protein processing. The full-length form of the HH protein (F) migrates with a mobility that corresponds to a relative molecular mass of 46-kD. This species is detected from in vitro translation extracts by Ab1 and Ab2 (Fig. 1, lanes 4 and 16), and is partially converted to a species of 39 kD (U) when translation occurs in the presence of microsomes (Fig. 1, lanes 5 and 17). A 39-kD species that comigrates with U is also present in extracts from all in vivo sources, but none of these extracts contains detectable levels of F. We conclude that U represents the signal-cleaved form of F; signal cleavage thus appears to be relatively inefficient in vitro (*3*) but is highly efficient in vivo (*18*).

In addition to signal cleavage, further cleavage of the U precursor generates other forms of HH protein that are observed in vivo. We deduce this from the observation that Ab1 and Ab2 both detect the U (uncleaved) species, but they also interact individually with smaller protein species that are expressed endogenously in embryos and imaginal disks and with species expressed on introduction of the *hh* gene into S2 cells. Ab1 thus interacts with a 19-kD species from all these tissues (Fig. 1, lanes 2, 3, 6, 8, and 9), whereas Ab2 interacts with a 25-kD species and with a 16-kD species (Fig. 1, lanes 14, 15, 18, 20, and 21). We refer to the 19-kD species as N (NH_2-terminal fragment), to the 25-kD species as C (COOH-terminal fragment), and to the 16-kD species as C*. These species represent the major forms of endogenous HH protein present in vivo (*19*).

The proposed cleavages by which these species arise are shown schematically in Fig. 1E. The N and C species are detected by Ab1 and Ab2, respectively, and the sum of the relative masses of the two smaller species is roughly equivalent to the relative mass of U (*20*). A simple mechanism that could account for the derivation of the two smaller species therefore, would be a single internal cleavage of the U precursor. Processing of the HH protein when translated in vitro also yields a 25-kD species (Fig. 1C) and either a 29-kD or 19-kD species (Fig. 1A). The 19-kD species comigrates with N, and its formation depends upon the presence of microsomes, consistent with the proposal that N derives from F by signal cleavage and a further internal cleavage. Also consistent with an internal cleavage, the relative mass of the 25-kD species that comigrates with C is not affected by the presence of microsomes. The overall pathway for formation of the predominant forms of HH protein observed in vivo thus appears to involve signal cleavage of F to generate U, which is then cleaved internally to form N and C, the predominant forms found in vivo. Further processing of the 25-kD C species might then generate the 16-kD C* species, but we cannot resolve whether this processing is a single cleavage event because Ab2 does not recognize the smaller 9-kD fragment that would result. The processing of C to generate C* appears to occur with greater efficiency in imaginal disks than in embryos (Fig. 1C), which may be the result of the mass isolation procedure used to obtain imaginal disks (*21*).

Autoproteolysis of the HH protein. The comigration of endogenous and in vitro–generated HH protein species suggested that in vitro processing is similar to

that observed in vivo. Our early in vitro work with a truncated form of the HH protein had suggested the possibility of autoproteolysis (*3*), but no sequence similarity to known proteases had been detected for HH or for any of the vertebrate homologs. However, a seven-residue region of HH coding sequence (residues 323 to 329 in the *Drosophila* protein) displays some similarity to the sequences of serine proteases (Fig. 2). This region lies approximately two-thirds of the distance from the signal cleavage site to the COOH-terminus, and includes Thr and His residues (positions 4 and 7 in Fig. 2), which are invariant among all HH sequences from all species. In the serine proteases, this conserved sequence contains an invariant His that acts as a general base in catalysis (*22*).

To determine whether this invariant His residue in the HH protein functions in autoproteolysis, we purified two proteins after production in *Escherichia coli*: one carried the wild-type sequence and the other contained a substitution of an Ala codon for the His codon at position 329 (H329A). Both of these proteins were engineered to contain a hexahistidine tag at the NH_2-terminus fused to *Drosophila* sequences that extend from a residue just before the signal cleavage site to the COOH-terminus (residues 83 to 471). The wild-type form of this protein is referred to as His_6-U. Both proteins were extensively purified under denaturing conditions with the use of a Ni^{2+}-chelating matrix (Fig. 3A). On dilution of denaturant, the wild-type protein (His_6-U), but not the H329A mutant protein (His_6-U_{H329A}), released a 25-kD species detectable by Ab2 and identical in mobility with the C species produced from in vitro translations and various in vivo sources (Fig. 3B). This cleavage was also observed when the wild-type protein was purified and renatured by other protocols and cleaved under distinct conditions (*23*). We therefore conclude that the HH protein can undergo autoproteolysis, and that the H329 residue is required for this activity.

To more precisely define the domain of the HH protein responsible for autoproteolysis, we examined the effects of several distinct types of mutations on in vitro processing. The most informative mutation was a deletion that removes residues 89 to 254 (Δ89-254), which together constitute most of the amino acids within the N fragment. This construct generates a full-length species with a mobility that corresponds to the expected relative mass of 33-kD, and two cleaved products, whose apparent relative masses (25 and 9 kD) sum to give the relative mass of the larger species (Fig. 4A, lane 2) (*24*). The larger of the two cleaved products comigrates with the C species produced from the wild-type protein, which suggests that the Δ89-254 HH protein contains the residues normally present in C, and all of the determinants required for autoproteolysis, including the normal cleavage site. We also conclude that most of the residues within N are dispensable for autoproteolytic activity.

In contrast, lesions that affect residues presumed to lie within C fail to undergo autoproteolysis in vitro (*25*). These mutations include the H329A mutation described above, a mutation that inserts an influenza viral epitope between residues 408 and 409 (flu408), and three mutations that cause premature termination of the protein at the COOH-terminus (*26*). The two most severe truncations, 294 trunc and 410 trunc, are mutations generated in vitro (*26*). They cause a loss of 177 and 61 residues, respectively, from the COOH-terminus of the protein, and neither undergoes

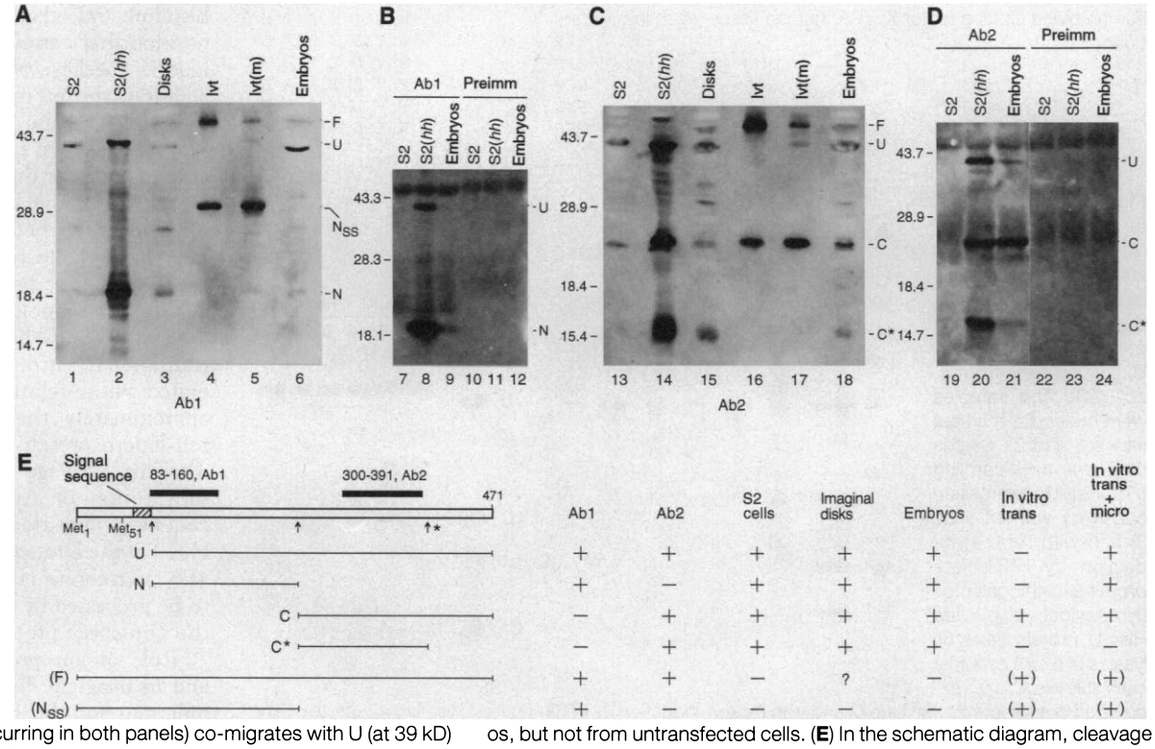

Fig. 1. Processing of the HH protein. (**A** and **C**) Immunoblots with antibodies to amino- (Ab1) and COOH-terminal (Ab2) epitopes (*42*). Lanes contain protein from induced untransfected S2 cells (lanes 1 and 13), transfected S2 cells induced to express HH (S2(*hh*); lanes 2 and 14) (*43*), imaginal disks (lanes 3 and 15), wild-type embryos (*44*) (lanes 6 and 18), and in vitro translations of synthetic *hh* mRNA both in the presence (lvt(m); lanes 5 and 17) and absence of microsomes (lvt; lanes 4 and 16) (*38*). Multiple species were detected, as illustrated in the schematic diagram below. Minor cross reactive bands are seen in most samples including extracts of induced untransfected S2 cells (lanes 1 and 13). One of these bands (occurring in both panels) co-migrates with U (at 39 kD) and is particularly abundant in lane 6 of (A). (**B** and **D**) Blots of samples immunoprecipitated with Ab1 [(B), (lanes 7 to 9)], Ab2 [(D), (lanes 19 to 21)], or preimmune serum [(B), (lanes 10 to 12)] and [(D), (lanes 22 to 24)]. Detection was with biotinylated derivatives of Ab1 (B) and Ab2 (D) (*45*). Samples used were: induced untransfected S2 cells, lanes 7, 10, 19, and 22; transfected S2 cells induced to express *hh*, lanes 8, 11, 20, and 23; and embryos, lanes 9, 12, 21, and 24. For either antibody, HH protein fragments were specifically immunoprecipitated from *hh* expressing cells and embryos, but not from untransfected cells. (**E**) In the schematic diagram, cleavage sites are denoted by arrows. The cleavage site marked by the asterisk is inferred by identification of only one cleavage product and may therefore occur at another location within the C fragment. The first two columns to the right of the diagram indicate the reactivity of Ab1 and Ab2 to each HH fragment. The other columns indicate the presence (+) or absence (−) of each HH fragment in the various samples. Parentheses around F and N_{SS} indicate that these species are detected in in vitro translation reactions but not in vivo.

proteolysis. The 456 trunc HH protein is like that encoded by the EMS-induced hh^{13E} mutant allele, which results in the loss of 15 residues from the COOH-terminus of the protein (*26*). This protein undergoes autoproteolysis, as demonstrated by the appearance of a 24-kD band in place of C, but the efficiency of the reaction is much impaired in vitro (Fig. 4B). We thus conclude that autoproteolysis of the HH protein relies mainly upon residues within C. Deletion or alteration of residues within this domain is associated with reduced efficiency of processing, and one such deletion appears to be the cause of the hh^{13E} mutation.

The sequence homology and autoproteolytic function of the HH protein suggested the possibility that the full-length (F or U) or the C fragment can act as a sequence-specific protease. As a first step in clarifying the mechanism of autoproteolysis, we introduced an influenza virus epitope tag (flu227) into the NH_2-terminus of a *hh* open reading frame that also carried a H329A mutation. The insertion of the epitope tag alone does not interfere with autoproteolysis (Fig. 4C, lane 9), and cleavage yields a normal C fragment and an N fragment of increased relative mass when compared to wild-type. The protein that carries both mutations does not undergo proteolysis (Fig. 4C, lane 10). Because the epitope-tagged N fragment migrates differently from N, the double mutant provides a substrate to look for intermolecular cleavage upon mixture with a wild-type sequence. In such a mixture, although normal N is formed, no tagged N can be detected (Fig. 4C, lane 11). Thus, in this experiment, no appreciable intermolecular cleavage occurs. We also did not detect intermolecular cleavage in the following two experiments: (i) co-transfection of wild-type and 410 trunc sequences into S2 cells (the cleaved 410 trunc protein would yield a smaller and therefore identifiable form of C) and (ii) mixing of excess unlabeled, purified His_6-U protein with labeled, in vitro translated H329A mutant protein. Thus, although we cannot rule out the possibility of an intermolecular mechanism for regulation of autoproteolysis or for cleavage of other proteins, our current evidence suggests that cleavage of the HH protein occurs predominantly by an intramolecular mechanism.

A

	1	2	3	4	5	6	7
D. mel. hh	L	T	V	**T**	P	A	**H**
D. hydei hh	L	T	V	**T**	P	A	**H**
C-Shh	L	L	L	**T**	A	A	**H**
M-Shh/Hhg-1	L	L	L	**T**	A	A	**H**
R vhh-1	L	L	L	**T**	A	A	**H**
Z-Shh/Zf vhh-1	I	T	L	**T**	A	A	**H**
twhh	L	T	L	**T**	A	A	**H**
M-Dhh	L	L	L	**T**	P	W	**H**
M-Ihh	L	A	L	**T**	P	A	**H**

B

CHT	W	V	V	T	A	A	H
TRP	W	V	V	S	A	A	H
ELA	W	V	M	T	A	A	H
UKH	W	V	I	S	A	T	H
C1R	W	I	L	T	A	A	H
C1S	W	V	L	T	A	A	H
MCP	F	V	L	T	A	A	H
FAX	Y	V	L	T	A	A	H
TPA	W	I	L	S	A	A	H

Fig. 2. Limited sequence similarity between HH proteins and serine proteinases. (**A**) HH protein sequences are aligned to residues 323 to 329 of the *D. melanogaster* protein and numbered as positions 1 to 7. Conserved HH residues are in bold letters. (**B**) The catalytic histidines (*22*) of mammalian serine proteinases are aligned to the invariant histidine at position 7 in HH proteins. Abbreviations are as follows: C-Shh, chicken Sonic hh (*9*); M-Shh, mouse Sonic hh (*10*) [identical to Hhg-1, (*15*)]; R vhh-1, rat vhh-1 (*12*); Z-Shh, zebrafish Sonic hh (*11*) [corresponds to shh (*27*) and zebrafish vhh-1 (*12*)]. twhh (*27*); M-Dhh, mouse Desert hh (*10*); M-Ihh, mouse Indian hh (*10*); CHT, bovine chymotrypsin; TRP, bovine trypsin; ELA, porcine elastase; UKH, human urokinase; C1R, human complement factor 1R; C1S, human complement factor 1S; MCP, rat mast cell protease; FAX, human blood clotting factor X; TPA, human tissue plasminogen activator.

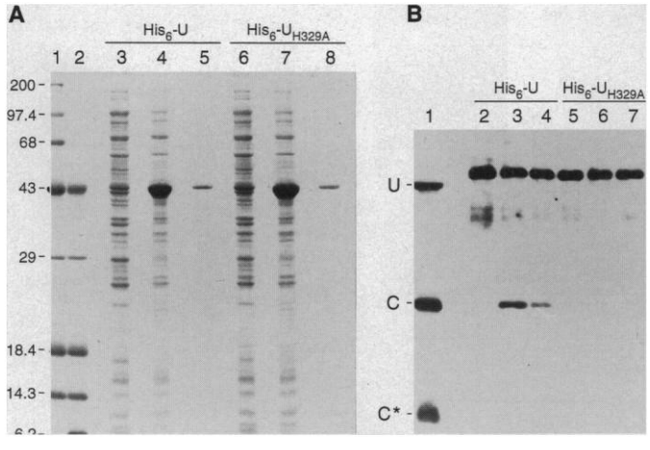

Fig. 3. Autoproteolysis of the HH protein. (**A**) Polyacrylamide gel stained with Coomassie blue that shows the production and purification of His_6-U and His_6-U_{H329A} proteins from *E. coli* (*23*). The samples were molecular markers (lanes 1 and 2); lysates of *E. coli* cells carrying the His_6-U expression construct without (lane 3) and with (lane 4) induction by IPTG (isopropyl-β-D-thiogalactopyranoside); purified His_6-U protein (lane 5); lysates of *E. coli* cells that carry the His_6U_{H329A} expression construct without (lane 6) and with (lane 7) induction by IPTG; purified His_6-U_{H329A} protein (lane 8). Purified proteins were essentially homogeneous except for several minor species of lower relative mass; these species are endogenous breakdown products of the full-length proteins because they were absent in uninduced extracts and were detectable with *hh* antibodies (*39*). (**B**) An immunoblot detected with Ab2 (*42*) showing transfected S2 cells induced to express *hh* (lane 1); His_6-U and His_6-U_{H329A} proteins incubated in cleavage reaction buffer (*23*) for 0 hours (lanes 2 and 5), for 20 hours (lanes 3 and 6), and for 20 hours in the presence of 20 mM TAME (a serine protease inhibitor) (lanes 4 and 7) (*46*). On incubation, the His_6-U, but not the His_6-U_{H329A} protein, released a fragment presumed to be C on the basis of reactivity with Ab2 and comigration with C produced in S2 cells. Release of C (lane 3) was only partially inhibited by TAME.

Role of autoproteolysis in embryonic and in imaginal disk signaling. Numerous functions for the *hh* gene have been described in *Drosophila*. At the morphological level these include a role in the patterning of larval cuticular structures and in the patterning of adult structures such as the eye and appendages (*1*, *2*, *3*, *8*, *13*, *14*). The mechanistic basis for these morphological effects involves signaling for maintenance or induction of gene expression in embryos

The *hh* gene has been broadly conserved throughout evolution, with single homologs being identified in various invertebrate species (*15*), and with multiple distinct homologs being found in each of several vertebrate species (*10–12*, *15*, *27*). All these HH protein sequences contain an invariant histidine and other conserved residues at a position that corresponds to the H329 residue in the *Drosophila* protein (Fig. 2). In addition, the protein encoded by at least one of the mouse *hh* genes appears to be processed in vivo to yield two smaller species in a manner that resembles the in vivo processing of the *Drosophila* protein (*15*). To determine whether autoproteolysis may also play a role in vertebrates, we examined the behavior of proteins encoded by two distinct *hh* homologs from the zebrafish, *twhh* and *shh*. When these sequences are translated in vitro, smaller species are generated whose relative masses sum to yield approximately the relative mass of the full-length protein (Fig. 4D, lanes 1 and 3). This cleavage reaction is blocked by substitution of Ala codons for the His codons at positions that correspond to H329 of the *Drosophila* protein (Figs. 2 and 4D). Vertebrate HH proteins thus appear to be processed by a similar mechanism as the *Drosophila* protein.

and imaginal disks (*3*, *8*, *13*, *15*, *28*–*32*). To ascertain the importance of autoproteolysis for these functions, the H329A mutant gene under control of the hsp70 promoter was introduced by P element–mediated transformation into the *Drosophila* germ line (*33*). Heat shock induction results in the formation of an abundant species that corresponds to U on the basis of its mobility and its interaction with Ab1 and Ab2 (Fig. 5, lanes 5 and 10). In contrast, induction of wild-type HH protein with the use of a similar construct resulted in similar amounts of the N and C processed products, with little uncleaved U (Fig. 5, lanes 4 and 9). Thus, as observed in vitro and in S2 cells, the H329A mutation in embryos appears to greatly reduce the efficiency of autoproteolytic cleavage of the HH protein.

Perhaps the earliest known requirement for HH protein is in maintenance of an adjacent stripe of *wingless* (*wg*) gene expression in each embryonic segment (*28*, *29*). This requirement is deduced from the loss of *wg* expression when *hh* function is absent; in addition, the ubiquitous expression of wild-type HH protein induces expansion of the domain of *wg* gene expression (*15*, *32*). We examined the effects of the H329A mutation on *wg* expansion by heat shocking embryos carrying the H329A mutant construct in parallel with embryos containing the wild-type construct. Although the H329A mutant protein is able to induce some expansion of the *wg* domain, the efficiency of this activity is impaired relative to that of the wild-type protein (Fig. 6, B and C, and Table 1). The difference in efficiency ranges nearly as high as threefold depending upon the heat shock regime (*33*), and these results suggest that autoproteolysis of the HH protein is important for optimal activity in embryonic signaling to induce *wg* expression.

The effects of HH protein on the patterning of cuticular structures are most clearly visible on the dorsal surface of the larva, where four distinctive cell types can be identified in each parasegment. These cell types have been designated 1°, 2°, 3°, and 4°, from anterior to posterior, with *hh* transcription occurring in precursors of the 1° cells (*14*). Differentiation of the first three cell types was shown to be dependent upon *hh* gene function, and it has been proposed that the fates of these cells are determined by the concentration of HH protein, with highest concentrations producing the 1° fate, intermediate concentrations producing the 2° fate, and the lowest concentrations producing the 3° fate (*14*). This proposal was supported by observations that the most anterior cell types display the greatest sensitivity to a reduction of *hh* expression, and that all of the 3° and some of the 4° bristles are replaced by naked cuticle characteristic of the more anterior 2° cell type when *hh* is expressed ubiquitously at high levels. We have reproduced suppression of 3° and some 4° fates by heat shock induction of embryos that carry our wild-type construct (Fig. 6E), but find that the H329A mutant is unable to alter cell fates in the dorsal cuticle of the larva (Fig. 6F). Autoproteolysis, or perhaps some other function blocked by the H329A mutation, thus appears to be essential for the patterning influence of HH protein upon the dorsal cuticle.

We have extended our examination of H329A mutant protein function to study its effect on the patterning of adult structures and signaling within imaginal disks. In the eye imaginal disk, *hh* function is required for the appropriate development of pattern (*2*–*4*) and more recently has been shown to control progression of a wave of differentiation by way of the induction of *decapentaplegic* (*dpp*) gene expression in the morphogenetic furrow of the eye (*30*, *31*). In leg and wing disks, ectopic expression of *hh* has

Table 1. Wild-type and mutant *hh* activity in embryonic induction of *wg* expression. Expansion of *wg* expression beyond wild-type controls is given as average number of cell diameters ± standard deviation with the number of embryos scored in parentheses.

	Expansion of *wg* expression after heat shock*			
	10 minutes	30 minutes	10+10†	30+30‡
hs*hh*	1.0 ± 0.3 (93)	1.5 ± 0.6 (120)	2.9 ± 0.3 (41)	2.8 ± 0.4 (54)
hs*hh* H329A	0.7 ± 0.5 (190)	0.9 ± 0.4 (111)	1.1 ± 0.4 (145)	1.9 ± 0.5 (93)

*See (*33*) for heat shock conditions. †Two 10-minute shocks were administered. ‡Two 30-minute shocks were administered.

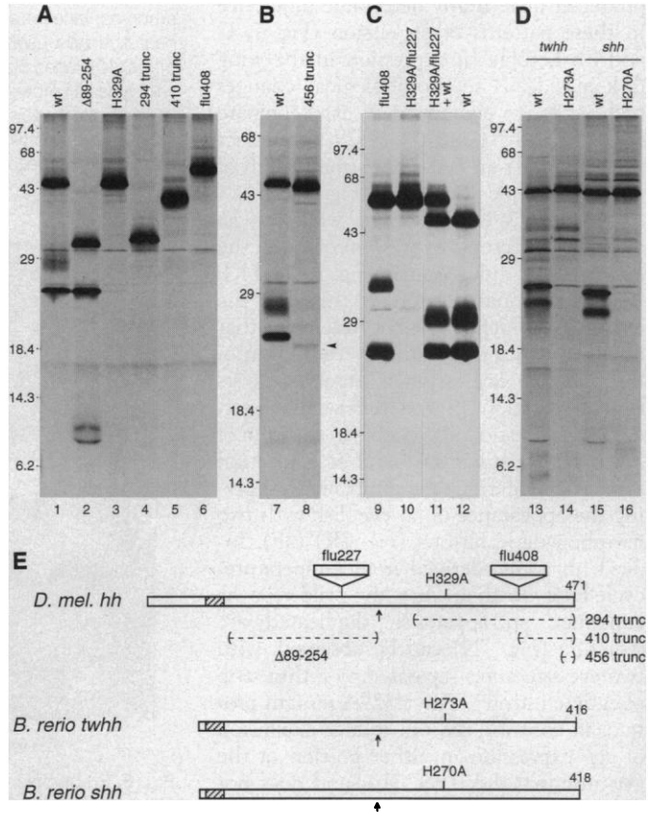

Fig. 4. Autoproteolytic functions of *Drosophila* and zebrafish HH proteins map to the COOH-terminal fragment. In vitro translations (*38*) of wild-type and mutant HH proteins from *Drosophila* (**A** to **C**) and zebrafish (**D**) are shown. The locations of mutations and cleavage sites (arrows) in these proteins are illustrated in (**E**). In the *Drosophila* protein (A, B, and C), autoproteolysis is blocked or severely inhibited by several mutations in the COOH-terminus (H329A, 294 trunc, 410 trunc, flu408, and 456 trunc), but is unaffected by a large deletion (Δ89-254) or insertion of a flu-tag epitope trimer (flu227) (*26*) in the NH_2-terminus. Autoproteolysis thus depends primarily on residues within the C fragment (sequences to the right of the cleavage site in the diagram below; see Fig. 1). Furthermore, the H329A/flu227 double mutant is not cleaved by wild-type protein in a mixing experiment (lane 11), suggesting an intramolecular mechanism for autoproteolysis. HH proteins encoded by the zebrafish genes *twhh* and *shh* (*27*) display a pattern of processing (D) similar to that of the *Drosophila* protein although the NH_2-terminal fragment of each zebrafish protein (23 kD for twhh and 22 kD for shh) has a lower apparent mass than the COOH-terminal fragment (25 kD for twhh and shh). This is the result of a shorter stretch of residues that precedes the signal sequences as compared to the *Drosophila* protein. Processing is blocked by H273A and H270A mutations in twhh and shh proteins, respectively (analogous to the H329A mutation in the *Drosophila* protein), which suggests that an autoproteolytic processing mechanism similar to that observed for the *Drosophila* protein is used.

also been shown to yield pattern duplications and defects and is associated with induction of ectopic expression of other signaling molecules normally expressed in a zone along the anterior-posterior compartment boundary (*8*, *13*).

For our studies of signaling in imaginal discs we utilized a thermal cycler to subject larvae carrying heat shock-inducible *hh* constructs to successive rounds of heat shock and recovery. We then examined the effects of temperature cycling upon expression of *dpp* and *wg* in imaginal discs by monitoring β-galactosidase expression from a reporter gene carrying *dpp* promoter sequences or from an enhancer detector P element inserted in the *wg* gene. The expression of *wg* normally occurs in a ventral sector of the leg disk along the anterior-posterior compartment boundary (Fig. 7A), whereas *dpp* is expressed in the dorsal portion of the disk along this boundary (Fig. 7D). Although thermal cycling of larvae carrying the wild-type *hh* gene produced abnormal leg disk morphology and extensive ectopic expression of both target genes (Fig. 7, B and E), the H329A construct produced little if any detectable difference in these patterns of expression (Fig. 7, C and F). Ectopic *hh* expression in the wing disk also leads to morphological changes and expanded expression of *dpp* (compare Fig. 7, G and H), but the H329A construct produced only an occasional small patch of anterior ectopic expression (Fig. 7I) (*34*).

Ubiquitous expression of wild-type *hh* also leads to ectopic expression of *dpp* in the eye-antennal disk (compare Fig. 7, J and K). In the antennal portion of this disk the expansion of *dpp* expression resembles that observed in leg disks. In the eye portion of the disk *dpp* expression is observed at its normal location in the furrow; however, ectopic expression also occurs in the form of a second dorso-ventral band at a location somewhat anterior to the furrow, thus giving the appearance of an eye disk with two morphogenetic furrows (Fig. 7K) (*35*). Indeed, in adults derived from temperature-cycled larvae that carry the wild-type *hh* construct, an apparently duplicated eye structure (Fig. 7N) can be observed, with two eye structures separated by a thin strip of cuticle (arrow). The H329A mutant protein, in contrast, did not induce expansion of *dpp* expression in either portion of the eye-antennal disk (Fig. 7L), and does not induce eye duplications or cuticle defects in the adult (Fig. 7O).

The experiments described thus far comprise multiple series of larvae subjected to 2 days of thermal cycling followed by immediate dissection for analysis of imaginal structures or further incubation at constant temperature for analysis of adult structures. Although the H329A protein appeared to have little activity in these experiments, the small patch of ectopic *dpp* expression induced in the wing disk (Fig. 7I, arrow) suggested that some residual activity remained. This suggestion was borne out in a similar experiment involving 3 days of cycling prior to dissection: the H329A protein clearly displayed some *dpp*-inducing activity in this experiment, presumably as a result of the higher amounts of protein that accumulated during the longer cycling period. The wing in particular, but also other imaginal disks, displayed low and variable amounts of ectopic *dpp* expression. This expression in all cases was far less extensive than that observed for the wild-type construct examined in parallel; furthermore, morphological deformations of the imaginal disks, although quite common with the wild-type protein, were extremely rare with the H329A protein. We conclude that, although its potency is greatly reduced relative to wild-type, the H329A protein retains at least some activity in early embry-

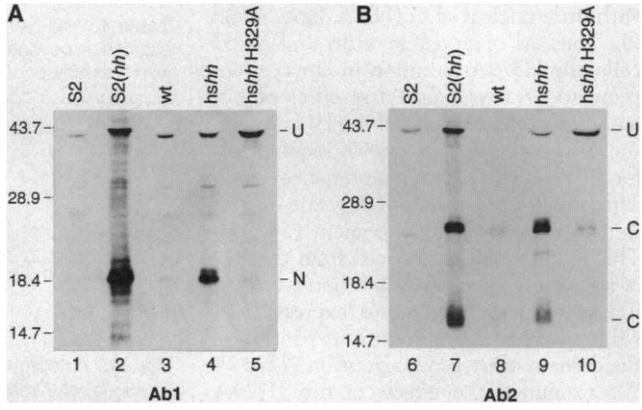

Fig. 5. Heat shock induced expression of wild-type and H329A mutant HH proteins in *Drosophila* embryos. (**A** and **B**) Immunoblots developed with Ab1 and Ab2, respectively (*42*, *44*). Lanes 1 and 6, induced untransfected S2 cells; lanes 2 and 7, transfected S2 cells induced to express *hh* (*43*); lanes 3 and 8, heat shocked for wild-type embryos; lanes 4 and 9, heat shocked hs*hh* embryos (*15*); lanes 5 and 10, heat shocked hs*hh* H329A embryos (*33*). In heat shocked hs*hh* embryos, the wild-type HH protein is both induced and properly processed to generate the U, N, C, and C* species seen in other expression contexts. In contrast, the H329A is induced but not appreciably processed in hs*hh* H329A embryos. The low amounts of processed species in lanes 5 and 10 are probably from endogenous *hh* expression because they are also the same in heat shocked wild-type embryos in lanes 3 and 8.

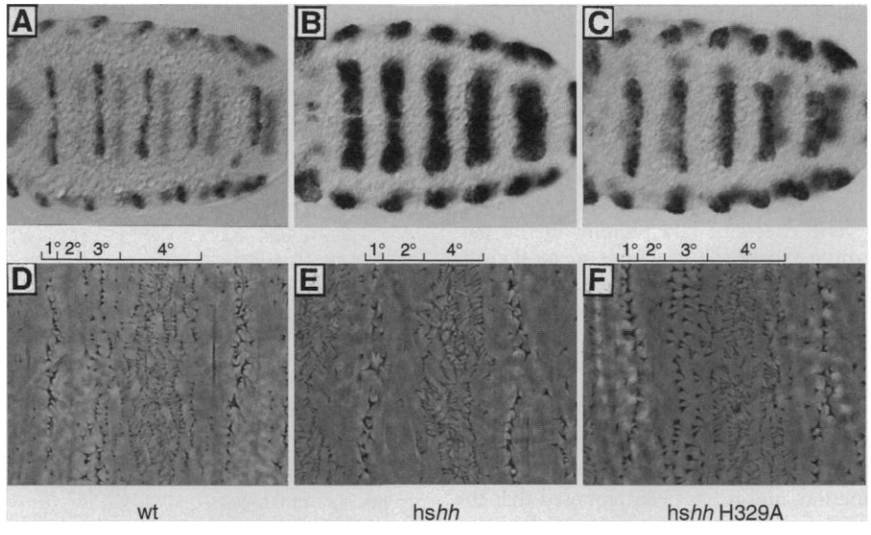

Fig. 6. Embryonic effect of ubiquitously expressed wild-type and H329A HH proteins. The embryonic distribution of *wingless* (*wg*) RNA as revealed by in situ hybridization is shown in (**A**) wild-type (homozygous $y^1\ w^{1118}$), (**B**) hs*hh*, and (**C**) hs*hh* H329A embryos that were exposed to two 10-minute heat shocks separated by a 90-minute recovery period (*33*). Wild-type embryos showed little change in *wg* expression, whereas the wild-type protein and, to a lesser extent, the H329A protein each induced ectopic *wg* expression (Table 1). Panels (**D**), (**E**), and (**F**) show the dorsal surfaces of $y^1\ w^{1118}$, hs*hh*, and hs*hh* H329A larvae, respectively, at the fourth abdominal segment. These larvae were shocked for 30 minutes as embryos and allowed to complete embryogenesis (*33*). Cuticle cell types (1°, 2°, 3°, and 4°) are labeled as described (*14*). The expansion of 2° cell types (naked cuticle) occurs at the expense of 3° and some 4° types in the hs*hh* embryo (E) under conditions in which the phenotype of hs*hh* H329A embryos (F) is identical to that of control embryos (D).

onic and imaginal disk induction of *wg* and *dpp* expression; in contrast, even under heat shock conditions far more severe than those required for effects by the wild-type protein, the H329A mutant remained completely inert with respect to the re-specification of cell fates in the dorsal cuticle of the larva.

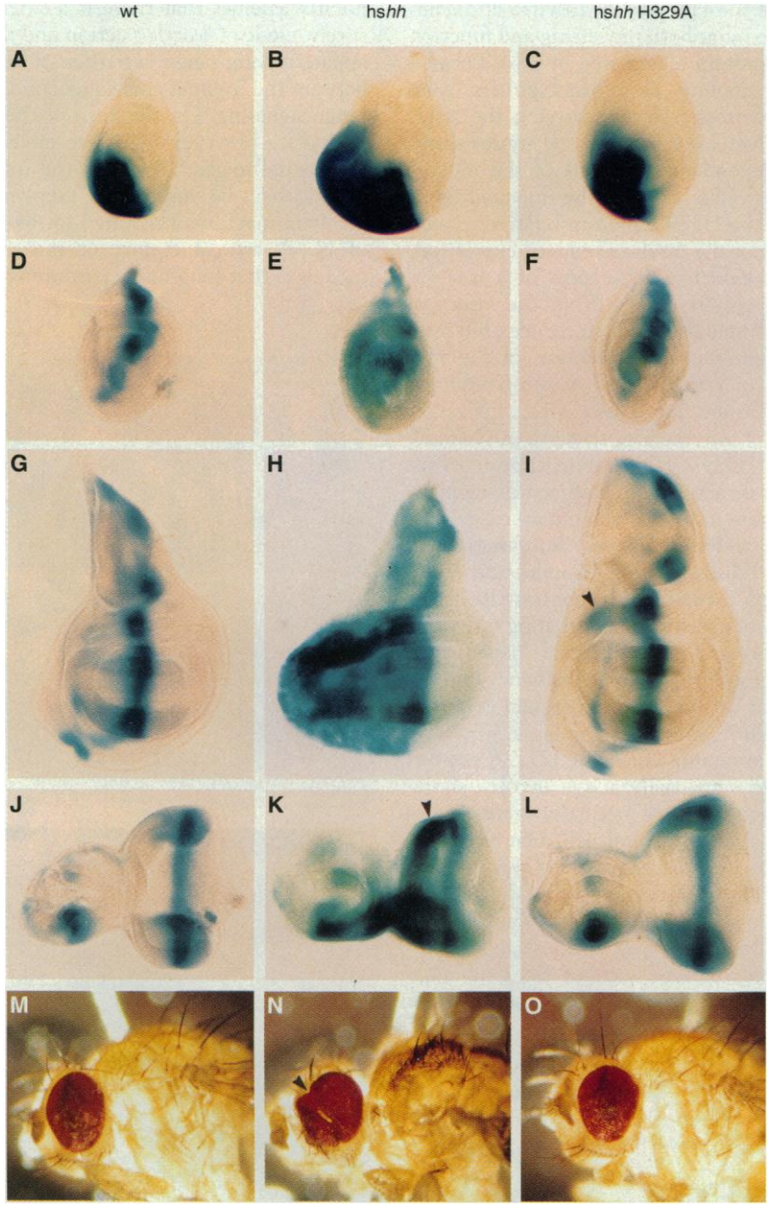

Fig. 7. Imaginal disk effects of ubiquitous wild-type and H329A HH proteins. X-gal staining was used to follow expression of *wg* (**A** to **C**) or *dpp* (**D** to **L**) in imaginal disks of late third-instar larvae that carry *wg-lacZ* or *dpp-lacZ* reporter genes (*47*). Leg (A to F), wing (G to I) and eye-antennal disks (J to L) from control larvae (A, D, G, and J), larvae carrying the hs*hh* transgene (B, E, H, and K) and larvae carrying the hs*hh* H329A transgene (C, F, I, and L) are displayed. In all panels anterior is to the left. Arrows highlight the following features: an ectopic patch of *dpp* expression in the anterior compartment of wing disks in hs*hh* H329A larvae (I); and an ectopic band of *dpp* expression in eye portion of the eye-antennal disk anterior to the morphogenetic furrow (marked by the other band of *dpp* expression more posteriorly) in hs*hh* larvae (K). Expansion into the anterior compartment of *wg* expression in leg disks, and *dpp* expression in leg and wing disks in hs*hh* larvae is similar to that described for the ectopic expression of *hh* (*8*, *13*). Morphological changes in the anterior compartment of leg (B and E) and wing disks (H) were also as described (*13*). In contrast, disks from hs*hh* H329A and control larvae showed very little change in *wg* and *dpp* expression, even under prolonged heat shock conditions and morphological changes were never observed. (**M** to **O**) The eye phenotypes of adult control (M), hs*hh* (N), and hs*hh* H329A (O) flies that were shocked during larval development in a manner similar to that of the imaginal disk experiments above. Duplicated eye structures were observed in hs*hh* flies, but never in hs*hh* H329A flies. The arrow in (N) points to a thin strip of cuticle between the two eye structures. Other deformities were also seen in hs*hh* flies (for example, compare the thorax in N to M).

Distinctive biochemical properties and embryonic localizations of N and C. As outlined in the introduction, a puzzling feature of *hh* function is its apparent short-range action in settings such as embryonic and imaginal disk signaling to *wg* and *dpp* (*16*), and longer range action in other settings, such as patterning of the dorsal larval cuticle (*17*). These observations and the existence of two major protein products in vivo prompted us to look for differences in the solubility or diffusibility of N and C expressed in S2 cultured cells. These proteins behave differently, with most of the N fragment remaining cell-associated and all, or nearly all, of C being released into the culture supernatant (Fig. 8, A and B).

One possible explanation for this differential behavior might be the association of the N fragment with extracellular matrix proteins on the surfaces of the S2 cells. Accordingly, we examined the relative affinity of these two proteins for heparin agarose (*36*), because heparin binding is a common property of proteins that associate with the extracellular matrix (*37*). Given the obvious difficulty in obtaining soluble N from cultured cells, in vitro translation in the presence of microsomes was used to generate soluble, labeled N and C. Treatment with heparin agarose beads depleted N but not C from these translation extracts (Fig. 8C), whereas treatment with unmodified agarose beads did not deplete either fragment. Furthermore, N but not C was retained on the heparin agarose beads even after extensive washing with a solution that contained 0.1 percent Triton X-100 and 150 mM NaCl (*38*); in contrast, neither fragment was retained by unmodified agarose. We thus conclude that N, but not C, binds tightly to heparin, and this behavior suggests that the low concentration of N released into culture supernatants may be the result of binding to the extracellular matrix. Another mechanism that might contribute to the differential release of N and C into culture supernatant would be the expression in S2 cells of a receptor for N but not for C. Our current data cannot distinguish these possibilities.

The differential release of N and C into cultured cell supernatants suggested that these fragments might also be differentially localized in embryos. In previously reported HH protein localizations, either antibodies specific for N epitopes or antibodies unable to distinguish between N and C were used (*7*, *8*). In accordance with these reports, Ab1, which is specific for N epitopes, reveals a segmentally localized distribution that is slightly broader (Fig. 9B) than that of the *hh* transcript at the same stage (Fig. 9A). Also consistent with these reports, we observed that N epitopes at later stages

accumulate in large punctate structures (39). Our analysis is focused on the earlier stage, when antibody staining is weaker but prior to the formation of the invaginations and grooves that later crease the epidermis and thereby complicate the interpretation. We also used Ab2 to detect C-specific epitopes with various fixation and staining procedures (33). Although detection of C epitopes above background is more difficult than for N, we consistently observed a segmentally modulated pattern, albeit with a broader distribution than that of N (Fig. 9C). This localization is also distinctive in that C epitopes at early or late stages are not found in the punctate structures characteristic of N.

The hh^{13E} mutation encodes a prematurely truncated protein in which 15 residues normally present at the COOH-terminus are missing. Because this protein displays a much reduced efficiency in autoproteolysis, we examined the distribution of C in this mutant background. The C epitopes in a homozygous hh^{13E} embryo (identified by absence of a marked balancer) (33) are distributed in a much tighter segmental pattern than in wild type (Fig. 9D). This localization resembles that of N, and we thus conclude that the broad distribution of C epitopes normally seen is altered in hh^{13E} by retention of the uncleaved precursor near the site of synthesis.

The role of autoproteolysis in biogenesis of active HH protein. We have demonstrated that in addition to signal cleavage, the HH protein undergoes autoproteolysis at an internal site in order to generate the predominant protein species observed in vivo. All or most of the amino acid residues required for this autoproteolysis function map to C, the COOH-terminal product of this internal cleavage. In an effort to determine the importance of autoproteolysis for function, we introduced a single residue mutation (H329A) that blocks autoproteolysis of the HH protein in vitro and demonstrated that both processing and function of this protein is impaired in vivo. Because similar amounts of induced protein were detected from a strain carrying the wild-type construct or from several strains carrying independent insertions of the mutant construct (Fig. 5) (39), the impaired function of the H329A protein relative to wild type is not the result of reduced expression. Further evidence in support of a role for autoproteolysis derives from the effect of the hh^{13E} mutation, which reduces, but does not eliminate, autoproteolysis of the HH protein in vitro (Fig. 4). Correspondingly, the hh^{13E} mutation is associated with a phenotype of intermediate strength in vivo (2).

The H329A HH protein appears to retain weak activity in embryonic signaling and is able to induce ectopic *wg* expression and, to a lesser degree, can function in imaginal disk signaling for induction of ectopic *dpp* expression. In contrast to its retention of at least some signaling functions in embryonic and imaginal tissues, the H329 protein is completely inert when assayed for the ability to reprogram cell fates in the dorsal cuticle of the larva.

The assays in which the H329A protein is active or partially active involve short-range signaling that normally occurs across one or at most several cell diameters (13, 15, 32). In contrast, the H329A protein fails to affect patterning of the dorsal cuticle, a long-range activity of *hh* that normally operates across most of the segment. Previous proposals to account for long-range patterning activities have suggested that *hh* expression induces other signaling molecules that are then responsible for executing the patterning functions (the signal relay model) (Fig. 10A) (9, 13). This model implicitly assumes that there is a single consistent mode of *hedgehog* action and that the apparent long-range activities of *hh* products are the indirect consequences of short-range signaling. On the basis of the distribution we observe, the active molecule in this model might be N, and the role of C would then be limited to supplying the catalytic machinery required for biogenesis of N. A critical feature of this class of models is that long-range patterning effects

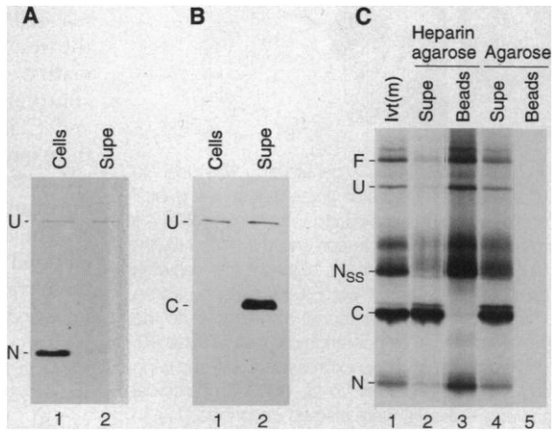

Fig. 8. Differential cellular release and heparin binding properties of N and C. (**A** and **B**) Immunoblots of sedimented cells (pellets) (lane 1) or supernatants (lane 2) from transfected S2 cell cultures expressing HH protein (43), developed with Ab1 (A) and Ab2 (B) (42). Samples in each lane were from the same volume of resuspended total culture. Whereas N remained mostly associated with the cell pellet (compare lanes 1 and 2 in A), C was nearly quantitatively released into the supernatant [compare lanes 1 and 2 in (B)]. U displayed partitioning properties in between those of N and C (A and B). (**C**) The heparin binding activity of various HH protein species generated by in vitro translations with microsomes (38). Samples were total translation mixture (lane 1); supernatant after incubation with heparin agarose or agarose (control) beads (lanes 2 and 4); and material eluted from heparin agarose or agarose beads after washing (lanes 3 and 5). F, U, N_{SS}, and N fragments are depleted from reactions incubated with heparin agarose but not agarose beads (compare lanes 2 and 4 to 1), and the same species subsequently can be eluted from the heparin agarose but not the agarose beads (compare lanes 3 and 5 with lane 1).

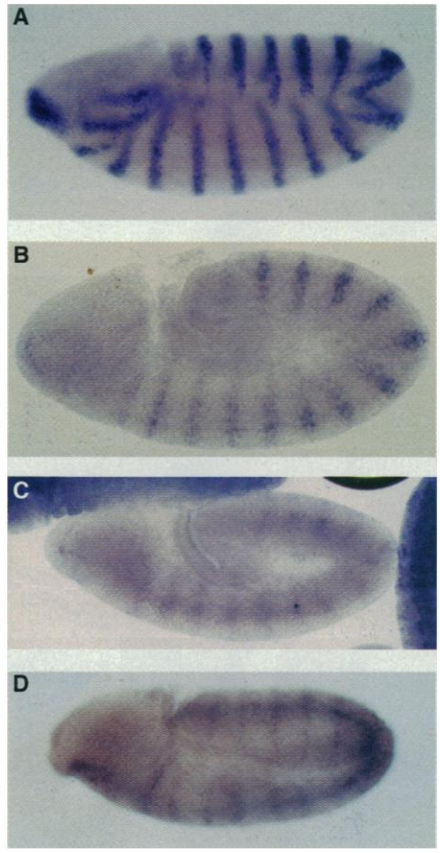

Fig. 9. Differential localizations of N and C in embryos. In situ localization of the *hh* transcript (**A**) is shown in comparison to the distribution of N and C epitopes detected with Ab1 and Ab2 in panels (**B**) and (**C**), respectively (33). The distribution of N and C epitopes span approximately one-third and one-half of each segmental unit respectively, whereas the transcript is limited to approximately one-quarter of each segmental unit. (**D**) The localization of C epitopes in embryos homozygous for the hh^{13E} allele is detected with the use of Ab2. In this mutant C epitopes, which displays impaired autoproteolytic activity, are more restricted, and resemble the wild-type localization of N. Homozygous hh^{13E} embryos were identified by loss of a marked balancer from a heterozygous parent stock (33). All embryos are at mid- to late stage 9 (extended germ-band).

of HH proteins should be reproducible on expression of another gene or genes whose expression normally would be induced by *hh*; no such function of other molecules has yet been demonstrated.

Our evidence suggests an alternative model, the dual function model (Fig. 10B), in which long- and short-range activities of the HH protein might be executed by N and C, the two predominant forms of the molecule observed in vivo. The nearly quantitative release of C fragment into the culture medium of *hh*-expressing S2 cells and its broad, though segmentally modulated distribution within embryos suggests that C might execute or contribute to long-range signaling functions. The N fragment, in contrast, predominantly remains associated with the expressing S2 cells and also binds to heparin, which suggests a possible association with the extracellular matrix. These properties and the segmentally restricted embryonic distribution of N are suggestive of a role in the execution of short-range *hh* signaling activities. Because the vertebrate HH proteins we tested also appear to be autoprocessed and also to carry predicted heparin binding sites just COOH-terminal to their signal sequence (*12*), many aspects of the dual function model discussed here in the context of *Drosophila* development may also apply to HH protein function in vertebrate development.

Execution of short-range functions by N would be consistent with the observation that the H329A mutant protein has at least partial function in signaling for the induction of *wg* and *dpp* because this mutation does not alter residues located in the NH_2-terminal portion of the protein that normally would give rise to N. The uncleaved H329A protein thus would carry all the residues that normally interact with a presumed receptor for N although there might be some effect on the affinity of the interaction as a result of the presence of COOH-terminal sequences, thus accounting for the decreased potency of the H329A protein (*40*). Execution of long-range functions by C is also consistent with our observations because long-range signaling might require the release of the C fragment or otherwise require the H329 residue for some function other than for autoproteolysis.

The signal relay and dual function models are not mutually exclusive, because each in turn may apply in different biological settings. Nor are these models the only possible explanations for *hh* function. For example, the uncleaved precursor U, although it is present in amounts significantly lower than N or C, may nevertheless play some role in long- or short-range *hh* signaling. In addition, other secreted molecules might be required for effective signaling. For example, long-range signaling by C might occur only in conjunction with other secreted proteins. Such additional factors could be constitutively expressed in many cell types and at many positions, or alternatively might be induced by other signaling proteins or by N. The latter possibility would actually combine aspects of the signal relay and dual function models.

A critical prediction of the dual function model is that constructs encoding N or C alone should be able to execute or contribute to distinct functions, whereas the signal relay model suggests that either N or C alone should be able to carry out all *hh*-associated functions. In support of the dual function model, experiments in vertebrate systems have demonstrated both long- and short-range activities for HH proteins (*12*, *41*), and recent evidence from work with a zebrafish *hh* gene indicates that N and C indeed do display distinguishable functions (*27*). Although further work is required to determine the operative mechanisms of *hh* signaling in *Drosophila*, our data clearly demonstrate that biogenesis of fully active HH protein requires an autoproteolytic cleavage event, and that the mechanism underlying this autoproteolysis appears to extend to vertebrate HH proteins.

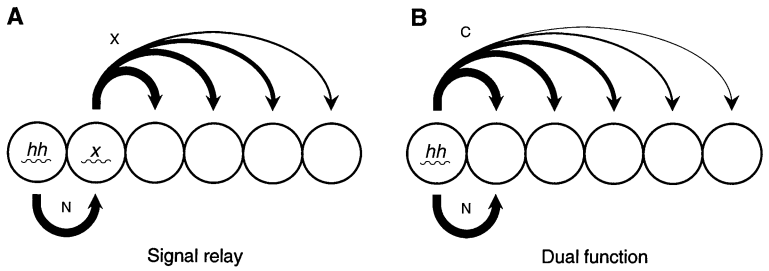

Fig. 10. Signal relay versus dual function models for HH protein action. (**A**) The long-range effects of *hh* signaling are achieved indirectly through short-range induction of a second signaling molecule (X). On the basis of its biochemical properties and its restricted tissue localization, N is presumed to represent the active short-range signal whereas the role of C would be limited to supplying the catalytic machinery required for biogenesis of N. (**B**) The long- and short-range signaling functions of *hh* are supplied by the N and C proteins derived by internal autoproteolysis of the U precursor. N is implicated in short-range signaling by retention near its cellular site of synthesis, while C is less restricted in its distribution and would execute long-range signaling functions. In both models, autoproteolysis is required to generate fully active signaling proteins.

REFERENCES AND NOTES

1. C. Nüsslein-Volhard and E. Wieschaus, *Nature* **287**, 795 (1980).
2. J. Mohler, *Genetics* **120**, 1061 (1988).
3. J. J. Lee, D. P. von Kessler, S. Parks, P. A. Beachy, *Cell* **71**, 33 (1992).
4. J. Mohler and K. Vani, *Development* **115**, 957 (1992).
5. T. Tabata, S. E. Eaton, T. B. Kornberg, *Genes Dev.* **6**, 2635 (1992).
6. S. Tashiro *et al.*, *Gene* **124**, 183 (1993).
7. A. M. Taylor, Y. Nakano, J. Mohler, P. W. Ingham, *Mech. Dev.* **42**, 89 (1993).
8. T. Tabata and T. B. Kornberg, *Cell* **76**, 89 (1994).
9. R. D. Riddle, R. L. Johnson, E. Laufer, C. Tabin, *ibid.* **75**, 1401 (1993).
10. Y. Echelard *et al.*, *ibid.*, p. 1417.
11. S. Krauss, J.-P. Concordet, P. W. Ingham, *ibid.*, p. 1431.
12. H. Roelink *et al.*, *ibid.*, p. 761.
13. K. Basler and G. Struhl, *Nature* **368**, 208 (1994).
14. J. Heemskerk and S. DiNardo, *Cell* **76**, 449 (1994).
15. D. T. Chang *et al.* *Development*, in press.
16. *hh* signaling in *Drosophila* embryos for maintenance of *wg* expression is limited to a range of one or two cells from the site of *hh* expression (*32*, *15*). Floor plate induction in neural tube explants is dependent upon direct contact with *hh*-expressing cells (*12*).
17. The expression of *hh* appears to influence *Drosophila* dorsal cuticle patterning over many cell diameters (*14*). The activity of *hh* appears to impose pattern upon the entire limb field (*9*, *15*).
18. To confirm that signal cleavage indeed is occurring at this unusual internal location, we introduced a mutation that changes residues S_{84} to N at the predicted signal cleavage site (*3*). This mutation prevents conversion by microsomes of F to U and also produces a species that comigrates with F upon transfection into cultured S2 cells (*19*). We also examined the effects of independently mutating the two methionine codons upstream of the signal sequence. In vitro translation of the sequence in which the first methionine is removed produces a protein species intermediate in mobility between F and U, and this species is converted to a species that comigrates with U in the presence of microsomes or when produced in vivo. Alteration of the second methionine codon caused no change in the electrophoretic mobility of HH protein produced in vivo or in vitro.
19. Smaller species of HH proteins from in vivo sources have been reported by J. Lee, D. von Kessler, and P. Beachy (1993 *Drosophila* Research Conference) and by (*8*). The latter study examined not endogenous proteins, but proteins induced to express at high levels from exogenously introduced constructs. The antibody did not distinguish epitopes from distinct portions of the molecule.
20. The electrophoretic mobilities of the F and U species are somewhat at variance with their predicted relative masses (52.1 and 43.3 kD, respectively). The identities of these species were confirmed by in vitro translation of various *hedgehog* open reading frames modified to contain different extents of sequence at the NH_2- or COOH-terminus (*18*, *39*), and by insertion of epitope tags (*39*). The migration anomalies appear to be associated with protein species in which sequences from both the NH_2- and COOH-terminal fragments are simultaneously present. The mobilities of the NH_2- and COOH-terminal fragments, in contrast, correspond to relative masses (19 and 25 kD, respectively) that sum to yield 44 kD, roughly equivalent to the expected relative mass of U.
21. O. M. Eugene, M. A. Yund, J. W. Fristrom, *Tissue Culture Assn. Man.* **5**, 1055 (1979).
22. A. J. Barrett, in *Proteinase Inhibitors* A. J. Barrett and G. Salvesen, Eds. (Elsevier, Amsterdam, 1986), pp. 3–22.
23. Plasmids encoding the His_6-U and His_6-U_{H329A} pro-

teins were generated by inserting sequences corresponding to residues 83 to 471 from the wild-type or *hh* H329A ORF into the pRSETB expression vector (Invitrogen). Proteins were induced in BL21(DE3)/pLysS *E. coli* cells as described [F. M. Ausubel *et al.*, *Current Protocols in Molecular Biology* [Wiley-Interscience, New York (1991)]. The basic purification was performed on Ni-NTA agarose beads (Qiagen) by a denaturing protocol with the use of 6 M guanidinium-HCl and 8 M urea essentially as recommended (a detailed protocol of exact conditions is available on request). Washing solutions contained 0.2 percent Tween 20 and 5 mM β-mercaptoethanol. The final washing buffer was: 6 M urea, 100 mM tris, 500 mM NaCl, 20 percent glycerol (pH 7.4). Elutions were performed with the final wash buffer containing 250 mM imidazole. In vitro cleavage reactions were performed by incubating the purified protein (diluted 1:30 in the final mix) in cleavage buffer [50 mM tris, 500 mM NaCl, 5 percent glycerol, 0.2 percent Triton X-100, 50 mM DTT (dithiothreitol), (pH 7.4)]. For the isolation of soluble full-length His_6-U protein free from denaturants or detergents, additional steps were taken (this refers to the other renaturation protocols mentioned in the text). Full-length protein from the eluate described above was further purified from breakdown products by precipitation, induced by urea removal through dialysis. The precipitate was again solubilized in a buffer containing guanidinium-HCl and placed on another Ni-NTA agarose column. After being washed as described, the protein was refolded (while attached to the beads) by gradual dilution of urea (from 6 M to 0.5 M) with dilution buffer [100 mM tris, 500 mM NaCl, 20 percent glycerol (pH 7.4)] over an 8-hour period at 4°C. The protein was eluted with dilution buffer containing 250 mM imidazole and 0.5 M urea. The eluate was dialyzed in 100 mM tris, 150 mM NaCl, 10 percent glycerol (pH 7.4) at 4°C and stored at −70°C.

24. The smaller of the cleaved products occasionally migrated as two bands (Fig. 4A). We have chosen the lower of the two bands between the 14.3- and 6.2-kD markers for our mass.
25. All mutations tested by in vitro translation were also examined in S2 cells by immunoblotting. In all cases the patterns of cleavage in S2 cells were identical to those observed in translations except that C* was always present whenever C was formed. The former fragment was not observed in translations.
26. All mutations in the *hh* gene were generated in the plasmid pF1 (*3*). Mutations in the zebrafish *twhh* and *shh* genes were generated with the original complementary DNA clones as described (*27*). All point mutations were generated with the use of recombinant circle polymerase chain reaction (PCR) [D. H. Jones and S. C. Winistorfer, *Biotechniques* **12**, 528 (1992)]. The flu408 and flu227 mutations were generated by inserting a trimer of the influenza hemagglutinin antigen (42 residues for flu408 and 43 residues for flu227) into the Alw NI and Bgl I sites present in the *hh* open reading frame (ORF) (nucleotide positions 1604 and 1058 respectively) (*3*). The Δ89-254 mutation was generated by removing sequences between the Eco NI site (644) and the Pml I site (1145). The 294 trunc mutation was generated by removing sequences between the Acc I site (1265) and the Xcm I site (1792). The 410 trunc mutation was previously generated and identified as HH_{410} (*3*). To map the mutation in the hh^{13E} allele (base change Cys^{1756} to Ala; coding change Tyr^{457} to STOP), DNA isolated from hh^{13E}/TM3 was used to seed PCR reactions generating regions of the hh ORF and flanking sequences, which were subcloned into Bluescript KSM (Stratagene). Six clones each, derived from two different PCR amplifications were sequenced.
27. S. C. Ekker, A. R. Ungar, P. Greenstein, D. P. von Kessler, R. T. Moon, P. A. Beachy, in preparation.
28. A. Martinez Arias, N. E. Baker, P. W. Ingham, *Development* **103**, 157 (1988).
29. S. DiNardo, E. Sher, J. Heemskerk-Jongens, J. A. Kassis, P. H. O'Farrell, *Nature* **332**, 604 (1988).
30. U. Heberlein, T. Wolff, G. Rubin, *Cell* **75**, 913 (1993).
31. C. Ma, Y. Zhou, P. A. Beachy, K. Moses, *ibid.*, p. 927.
32. P. W. Ingham, *Nature* **366**, 560 (1993).
33. The hs*hh* H329A construct was made identical to the hs*hh* construct (*15*) with the use of a *hh* ORF fragment containing the H329A mutation. Transgenic flies were generated from a $y^1\ w^{1118}$ parental strain according to the standard methods of P element–mediated transformation [A. C. Spradling and G. M. Rubin, *Science* **218**, 341 (1982)]. A line, HA3, carrying the hs*hh* H329A P element on the second chromosome was maintained as a homozygous stock. To assay for expansion of *wg* stripes, embryos collected 4 to 6 hours after egg laying (AEL) at 25°C were subjected to the following heat shock protocols before fixation. Embryos receiving single shocks (10 or 30 minutes at 37°C) were allowed to recover for 1 hour at 25°C. Embryos receiving double shocks (two 10-minute or two 30-minute shocks at 37°C) were allowed to recover 90 minutes after the first shock and 40 minutes after the second (Both recoveries were at 25°C. The double 30-minute protocol was as described; *11*). In situ hybridizations were performed as described [D. Tautz and C. Pfeifle, *Chromosoma* **98**, 81 (1989)] with a *wg* specific probe (*15*). Embryos assayed for cuticle phenotype were heat-shocked 6 to 8 hours AEL for 30 minutes at 37°C, allowed to develop at 25°C for 36 hours and then processed and mounted as described [M. Ashburner, Drosophila: *A Laboratory Manual* (Cold Spring Harbor Laboratory, Cold Spring Harbor, NY, 1989)]. Immunolocalizations (single or double stains) were performed as described [N. H. Patel, in *Imaging Neuronal Subsets and Other Cell Types in Whole Mount* Drosophila *Embryos and Larvae Using Antibody Probes*, in *Methods in Cell Biology*, L. S. B. Goldstein and E. Fyrberg, Eds. (Academic Press, New York, in press)]. Affinity-purified Ab1 or Ab2 (*45*) was used for the primary antibody and alkaline phosphatase (AP) or horseradish peroxidase (HRP)–conjugated antibody to rabbit or mouse immunoglobulin G (IgG) (Jackson Immunoresearch) was used for the secondary. Embryos from a hh^{13E}/TM3 *ftz*-lacZ (the balancer chromosome was from the Bloomington Stock Center, strain 3218) stock homozygous for the hh^{13E} allele were identified by the lack of staining with an antibody to β-galactosidase (Promega) in a double stain with Ab2 (Fig. 9D). Staining in Fig. 9, B and C, was performed on formaldehyde-fixed Canton-S embryos with the use of an AP-conjugated antiserum to rabbit IgG (secondary). Although standard formaldehyde fixation was generally used, heat and acid-formaldehyde fixation gave similar results.
34. Similar effects of ectopic wild-type *hh* expression in leg and wing imaginal disks have been reported (*8*, *13*), with ectopic expression resulting from a distinct method of induction or from a regulatory mutation. In theirs and our experiments, ectopic wild-type *hh* expression affected disk morphology and gene expression only in the anterior portions of leg and wing disks. This was not surprising because *hh* expression occurs in the posterior compartments of these disks without induction (*3*).
35. In eye disks, areas ectopically expressing *dpp* varied in size, presumably as a result of the induction of ectopic *hh* expression at varying time points during eye morphogenesis.
36. A heparin binding motif following the signal sequence in vhh-1 proteins from rat and zebrafish has been suggested (*12*).
37. A. D. Cardin and H. J. Weintraub, *Arteriosclerosis* **9**, 21 (1988).
38. In vitro translations were performed with the use of the TNT coupled transcription-translation system (Promega). [^{35}S]Methionine (DuPont NEN) was used for detection by autoradiography. In the heparin binding experiment (Fig. 8C), in vitro translation lysate with microsomes that produce wild-type HH protein was added to heparin agarose (Sigma) or Sepharose CL-4B (Pharmacia) beads that had been equilibrated with heparin binding buffer [HBB; 20 mM tris (pH 7.4), 150 mM NaCl, 0.1 percent Triton X-100]. Samples were incubated at 4°C for 4 hours with gentle rocking. After centrifuging the beads, supernatants in some samples were analyzed (lanes 2 and 4). The beads were then washed five times with chilled HBB and samples (lanes 3 and 5) were subsequently eluted at 80°C for 10 minutes in SDS–polyacrylamide gel electrophoresis (PAGE) loading buffer [F. M. Ausubel *et al.*, *Current Protocols in Molecular Biology* (Greene and Wiley-Interscience, New York, 1991)].
39. D. P. von Kessler, J. J. Lee, P. A. Beachy; unpublished data.
40. Alternatively, the partial function of H329A protein may derive from an extremely small fraction of protein that appears to be cleaved, since a very faint band with identical mobility to C appears in in vitro translations with the H329A protein (Fig. 4, lane 3).
41. C.-M. Fan and M. Tessier-Lavigne, *Cell*, in press.
42. Immunoblots were performed with affinity-purified Ab1 or Ab2 (*45*) by either of two chemiluminescence based protocols. In the first protocol (used in Figures 1, 3, and 5) samples were resolved by electrophoresis on 15 percent or 12 percent SDS-polyacrylamide gels [F. M. Ausubel *et al.*, *Current Protocols in Molecular Biology* (Greene and Wiley-Interscience, New York, 1991)] and transferred to Magnagraph nylon membranes (MSI) by electroblotting. Blots were developed with the use of an alkaline phosphatase–conjugated donkey anti-rabbit IgG secondary antibody and Lumi-Phos 530 (Boehringer Mannheim) under recommended conditions. In the second protocol (used in Fig. 8), samples were transferred to nitrocellulose filters (Schleicher and Schuell), and blots were developed using ECL reagents (Amersham) as recommended. The secondary antibody in this case was horseradish peroxidase conjugated goat anti-rabbit IgG (Jackson ImmunoResearch).
43. Complementary DNAs encoding various HH protein species were cloned into the pMK33 vector, which allows for inducible expression under metallothionein promoter control [M. R. Koelle *et al.*, *Cell* **67**, 59 (1991)]. Stable S2 cell lines were made by transfection of the *hh*/pMK33 plasmids with constant selection for hygromycin resistance. Proteins were expressed by plating a log phase culture of cells diluted to 0.1 A_{595} units, waiting 48 hours, inducing with $CuSO_4$ at 0.2 mM final concentration, and harvesting the cells or supernatant or both 24 hours later. Cell samples for immunoblotting were made by adding 10 volumes of 1× SDS-PAGE loading buffer (*38*) to pelleted cells. Cell pellets shown in Fig. 8, A and B, were washed once with media before preparation for immunoblotting.
44. Embryos from the wild-type Canton-S line and from the matings, hs*hh*/hs*hh* or hs*hh* H329A/hs*hh* H329A X *y*; *Sco/CyO*, *enlacZ11::wg* [J. A. Kassis, E. Noll, E. P. VanSickle, W. F. Odenwald, N. Perrimon, *Proc. Natl. Acad. Sci. U.S.A.* **89**, 1919 (1992)], were collected 0 to 16 hours after egg laying (AEL) at 25°C. They were heat shocked for 30 minutes at 37°C and allowed to recover for 1 hour at 25°C. Embryos in Fig. 1 (Canton-S) were collected 4 to 8 hours AEL at 25°C. In preparation for immunoblotting, all embryos were dechorionated in 2.6 percent sodium hypochlorite and homogenized in 10 volumes of 1X SDS-PAGE loading buffer (*38*).
45. GST fusion proteins containing either residues 83 to 160 or 300 to 391 from the HH protein were expressed in *Escherichia coli*, purified as recommended [F. M. Ausubel *et al.*, *Current Protocols in Molecular Biology* (Greene and Wiley-Interscience, New York, 1991)], and used to immunize rabbits by standard methods. The antibodies were affinity purified on a column of His_6-U protein [E. Harlow and D. Lane, *Antibodies: A Laboratory Manual* (Cold Spring Harbor Laboratory, Cold Spring Harbor, NY, 1988)] linked to Affi-Gel 10 beads (Bio-Rad). The purification was performed as described (Harlow and Lane) except that the acid and base elutions contained 10 percent dioxane. Biotinylated *hh* antibodies were prepared by purifying the rabbit antisera over a protein A column, followed by biotinylation with the use of the Immunoprobe biotinylation kit (Sigma). Immunoprecipitations were performed as described [Harlow and Lane] with the use of cold RIPA lysis buffer containing 0.25 mM phenylmethylsulfonyl fluoride (PMSF) and 5 mM EDTA for tissue homogenization. Lysates were precleared twice with pre-immune rabbit serum plus protein A beads (Gibco-BRL). Affinity-purified antibodies or preimmune serum was then added, and the immunoprecipitation was performed with protein A beads, with the use of NP-40 lysis buffer for the washes.
46. We have performed preliminary proteinase inhibitor

studies on in vitro translated HH protein by adding various inhibitors at the start of the translation reaction. These studies have been complicated by the fact that numerous protease inhibitors lower or block translation efficiency. In some cases we have assayed the effectiveness of an inhibitor by determining if addition of an inhibitor to a completed translation reaction will inhibit the self-processing that normally continues to occur. At this time we can only state the following with certainty: (i) the serine protease inhibitor TAME (*p*-toluenesulfonyl-L-arginine methyl ester) inhibits auto-proteolysis of in vitro–translated HH protein; (ii) soybean trypsin inhibitor, α_1 anti-trypsin, aprotitin, leupeptin, and E-64 do not block auto-proteolysis of translated HH protein; and (iii) TAME partially inhibits auto-proteolysis of purified His_6-U protein (Fig. 3, panel B).

47. Virgin female flies from the homozygous lines hs*hh* (15), hs*hh* H329A, and y^1 w^{1118} were crossed to males from the homozygous BS3.0 line (bearing a P element *dpp* reporter construct on the second chromosome, referred to as *dpp-lacZ* in the text) [R. K. Blackman, M. Sanicola, L. A. Raftery, T. Gillevet, W. M. Gelbart, *Development* **111**, 657 (1991)] or the line *y*; *Sco/CyO*, *enlacZ*11::*wg* (bearing a *wg* reporter P element enhancer trap on a second chromosome balancer; called *wg-lacZ* in the text) [J. A. Kassis, E. Noll, E. P. VanSickle, W. F. Odenwald, N. Perrimon, *Proc. Natl. Acad. Sci. U.S.A.* **89**, 1919 (1992)]. Progeny were grown at 25°C in aerated 0.5-ml microcentrifuge tubes containing yeast paste until the late second instar or early third instar stage of larval development. The larvae were then cycled continuously at 37°C for 30 minutes followed by 25°C for 90 minutes in a Perkin-Elmer thermal cycler until they reached the late third instar stage. They were subsequently dissected and stained with X-gal as described [M. Ashburner, Drosophila: *A Laboratory Manual* (Cold Spring Harbor Laboratory, Cold Spring Harbor, NY, 1989)] or allowed to grow to adulthood for phenotypic analysis.

48. We are grateful to D. Hursh and J. Kassis for fly stocks; A. Hammonds for imaginal disk tissue; D. Andrew and M. Heck for embryo collections; J. Ptak and C. Davenport for oligonucleotide synthesis; C. Berkower for a plasmid containing the flu tag epitope trimer; K. Young for advice on protein purification; and P. Roehm and D. Jackson for proofreading the manuscript.

7 September 1994; accepted 9 November 1994